

Minimal Neutrino Texture with Neutrino Mass Ratio and Cabibbo Angle

Yusuke Shimizu^{1,*}, Ryo Takahashi^{2,†} and Morimitsu Tanimoto^{1,‡}

¹*Department of Physics, Niigata University, Niigata 950-2181, Japan*

²*Department of Physics, Faculty of Science, Hokkaido University,
Sapporo 060-0810, Japan*

Abstract

We present neutrino mass matrix textures in a minimal framework of the type-I seesaw mechanism where two right-handed Majorana neutrinos are introduced in order to reproduce experimental results of neutrino oscillations. The textures can lead to experimentally favored leptonic mixing angles described by the tri-bimaximal mixing with one additional rotation. We present minimal and next to minimal textures for the normal mass hierarchy case in a context of the texture zero. A minimal texture in the inverted hierarchy case is also constructed, which does not have any vanishing entries in a Dirac neutrino mass matrix. We also discuss some cases that model parameters in the textures are supposed to be a neutrino mass ratio and/or the Cabibbo angle. Predicted regions of mixing angles, a leptonic CP-violation parameter, and an effective mass for the neutrino-less double beta decay are presented in all textures.

*E-mail address: shimizu@muse.sc.niigata-u.ac.jp

†E-mail address: takahashi@particle.sci.hokudai.ac.jp

‡E-mail address: tanimoto@muse.sc.niigata-u.ac.jp

1 Introduction

Neutrino oscillation experiments have revealed the lepton flavor to be large mixing, which are completely different from the quark mixing. Especially reactor experiments have observed a non-zero θ_{13} , which is the last mixing angle of lepton sector [1]. Now neutrino oscillation experiments go into a new phase of precise determinations of lepton mixing angles and neutrino mass squared differences [2, 3, 4]. Therefore, precise predictions are required for theoretical studies of neutrino mixing angles and neutrino mass ratios.

Before the reactor experiments reported the non-zero value of θ_{13} , we had a paradigm of "tri-bimaximal mixing" (TBM) [5, 6], which is a simple mixing pattern for leptons and can be easily derived from flavor symmetries. Actually many authors have discussed the TBM by introducing non-Abelian discrete flavor symmetries [7, 8]. However, the non-vanishing θ_{13} forces to study a deviation from the TBM [9, 10] or other patterns of lepton mixing angles, e.g. tri-bimaximal-Cabibbo mixing [11].¹

Now it is necessary to obtain simple textures of a neutrino mass matrix in order to investigate the origin of lepton mixing angles with the non-zero θ_{13} . Since the exact TBM cannot explain the current results of neutrino oscillation experiments, we consider two patterns of deviation from the TBM, which are defined by an additional rotation of 1-3 or 2-3 generation to the TBM.² These two patterns give a different prediction for the magnitude of $\sin^2\theta_{12}$. The additional 1-3 rotation strictly leads to $\sin^2\theta_{12} > 1/3$. On the other hand, in the case of 2-3 rotation, the additional rotation can give rise to $\sin^2\theta_{12} < 1/3$, which is in favor for experimental results. Therefore, we will focus on the additional 2-3 rotation to the TBM.

In this paper, we show how to derive the desired neutrino mixing pattern in a context of the type-I seesaw mechanism [13], which can give a natural realization of tiny neutrino masses compared to masses of other standard model (SM) fermions, with three generations of right-handed Majorana neutrinos in addition to three flavors of left-handed Majorana neutrinos in the SM. The presence of three generations of right-handed Majorana neutrinos are required for a gauge anomaly cancellation when one introduces a gauged $U(1)_{B-L}$ symmetry as a physics beyond the SM, e.g. SO(10) grand unified theory where the right-handed Majorana neutrinos can be naturally embedded. Models with three right-handed Majorana neutrinos are also well motivated for simultaneous explanations of important unsolved mysteries in the current particle physics and cosmology. They are, for example, a generation of baryon asymmetry of the Universe (BAU), to give a dark matter (DM) candidate, and an explanation of LSND/MiniBOONE anomaly in addition to a realization of the tiny neutrino masses (e.g. see [14]-[18]). It is known that in scenarios including a keV sterile neutrino DM, one of three right-handed Majorana neutrinos (which is a DM candidate with the mass of keV) should not affect the active neutrino masses in order to satisfy cosmological bounds. Therefore, we can effectively write down the right-handed Majorana neutrino mass matrix M_R and the Dirac neutrino mass matrix M_D in terms of sub-matrices in some scenarios including three generations of the right-handed Majorana neutrinos (one of them is a DM candidate) as

¹ See also [12] for a discussion of deviation from the TBM and a quark-lepton complementarity in a model independent way.

²A rotation of 1-2 generation still leads to $\theta_{13} = 0$, which has been just ruled out by the recent neutrino oscillation results.

follows:

$$M_R^{3 \times 3} = \begin{pmatrix} M_R^{1 \times 1} & 0 \\ 0 & M_R^{2 \times 2} \end{pmatrix}, \quad M_D = (Y_D^{3 \times 1} \quad Y_D^{3 \times 2}) v, \quad (1)$$

where $M_R^{1 \times 1}$ is the right-handed Majorana neutrino mass, which is the keV scale in the sterile neutrino DM scenario, $M_R^{2 \times 2}$ is a 2×2 right-handed Majorana neutrino mass matrix, $Y_D^{3 \times 1}$ is a 3×1 Dirac neutrino Yukawa matrix among the SM and the right-handed Majorana neutrino with mass of $M_R^{1 \times 1}$, $Y_D^{3 \times 2}$ is a 3×2 Dirac neutrino Yukawa one, and v is a vacuum expectation value (VEV) of the SM Higgs, respectively. Here, note that structures of mass spectrum and Yukawa matrix given in the Eq. (1) are naively splitting. Such kind of split mass spectrum and Yukawa matrix can be naturally realized in a split seesaw mechanism [16], Froggatt-Nielsen mechanism [19, 20], or a flavor symmetry [21]. Then, by using the seesaw mechanism, the left-handed Majorana neutrino mass matrix can be separately given as,

$$M_\nu = \left[Y_D^{3 \times 2} (M_R^{2 \times 2})^{-1} (Y_D^{3 \times 2})^T + Y_D^{3 \times 1} (M_R^{1 \times 1})^{-1} (Y_D^{3 \times 1})^T \right] v^2. \quad (2)$$

It is well known that an introduction of two right-handed Majorana neutrinos is a minimal scheme in order to reproduce the experimental data of three leptonic flavor mixing angles and two mass squared differences of the neutrinos [22]-[30]. Such situation can be embedded into the above scenario described by the Eqs. (1) and (2) without the loss of generality. For instance, if one consider the lightest sterile neutrino $M_R^{1 \times 1}$ as a candidate of the DM with the keV mass, the second term of the Eq. (2) does not affect the flavor mixing and the neutrino masses.³ Therefore, only the first term of the Eq. (2) contributes to the mixing and the masses. In other words, the neutrino flavor mixing is determined by only the structures of the 3×2 Dirac neutrino mass matrix and the 2×2 right-handed Majorana neutrino one. As the consequences, the lightest left-handed Majorana neutrino mass is very tiny compared with the other ones. In these setup, we will investigate the neutrino mass matrix texture which can reproduce the current neutrino oscillation experiments containing the result of the non-zero θ_{13} .⁴

The paper is organized as follows. We discuss some patterns of the deviation from the TBM in section 2. In section 3, we construct the minimal texture leading to the additional 2-3 rotation to the TBM. Finally, we present some specific cases of the minimal texture where model parameters are taken as the ratio between two mass squared differences of the neutrinos and/or the Cabibbo angle in section 4. Section 5 is devoted to the summary.

2 Deviations from the tri-bimaximal mixing

Mixing matrix for quarks and leptons is independently given by different unitary matrices including three mixing angles θ_{ij} ($i, j = 1, 2, 3; i < j$) and one Dirac phase δ . One of

³There is another option, i.e. one of the sterile neutrinos are super-heavy compared with the other two ones. Also in the case, such a super-heavy sterile neutrino does not contribute to the flavor mixing angles and two mass scales of the neutrinos since the sterile neutrino is decoupled from the theory at a high energy.

⁴See also [31] for discussions of the flavor mixing in the context of the split seesaw mechanism.

well-known parameterization of the mixing matrix is the PDG one [32] described as

$$\begin{aligned}
U &\equiv \begin{pmatrix} 1 & 0 & 0 \\ 0 & c_{23} & s_{23} \\ 0 & -s_{23} & c_{23} \end{pmatrix} \begin{pmatrix} c_{13} & 0 & s_{13}e^{-i\delta} \\ 0 & 1 & 0 \\ -s_{13}e^{i\delta} & 0 & c_{13} \end{pmatrix} \begin{pmatrix} c_{12} & s_{12} & 0 \\ -s_{12} & c_{12} & 0 \\ 0 & 0 & 1 \end{pmatrix} \\
&= \begin{pmatrix} c_{12}c_{13} & s_{12}c_{13} & s_{13}e^{-i\delta} \\ -s_{12}c_{23} - c_{12}s_{23}s_{13}e^{i\delta} & c_{12}c_{23} - s_{12}s_{23}s_{13}e^{i\delta} & s_{23}c_{13} \\ s_{12}s_{23} - c_{12}c_{23}s_{13}e^{i\delta} & -c_{12}s_{23} - s_{12}c_{23}s_{13}e^{i\delta} & c_{23}c_{13} \end{pmatrix}, \tag{3}
\end{aligned}$$

where c_{ij} and s_{ij} denote $\cos\theta_{ij}$ and $\sin\theta_{ij}$, respectively. Throughout this work we focus only on the lepton mixing matrix, namely Pontecorvo-Maki-Nakagawa-Sakata (PMNS) matrix U_{PMNS} [33, 34]. If neutrinos are Majorana particles, Majorana phases are included in the left-handed Majorana neutrino masses. For the leptonic mixing matrix, Harrison-Perkins-Scott proposed a simple form of the mixing pattern, so-called the tri-bimaximal mixing (TBM) [5, 6], as

$$V_{\text{TBM}} = \begin{pmatrix} \frac{2}{\sqrt{6}} & \frac{1}{\sqrt{3}} & 0 \\ -\frac{1}{\sqrt{6}} & \frac{1}{\sqrt{3}} & -\frac{1}{\sqrt{2}} \\ -\frac{1}{\sqrt{6}} & \frac{1}{\sqrt{3}} & \frac{1}{\sqrt{2}} \end{pmatrix}, \tag{4}$$

before reporting the non-vanishing θ_{13} . This TBM matrix reads

$$|U_{e2}| = \frac{1}{\sqrt{3}}, \quad |U_{e3}| = 0, \quad |U_{\mu 3}| = \frac{1}{\sqrt{2}}. \tag{5}$$

Since the TBM pattern is suggestive for studies of flavor physics behind the SM, a large number of works have been proposed for the realization of the TBM. However, the TBM has been just excluded due to the recent experimental result of the non-vanishing θ_{13} [1]. Therefore, one should consider alternatives of the TBM to reproduce the experimental results. One of the simple direction to explain the experimental data might be to minimally extend the TBM. The first task in this direction is to realize the non-zero θ_{13} because the experimentally observed mixing angles of θ_{12} and θ_{23} are still well approximated by the TBM.

In order to get the non-zero θ_{13} , one can consider an additional rotation of 1–3 generation. With this additional rotation, the PMNS mixing matrix can be written as

$$U_{\text{PMNS}} = V_{\text{TBM}} \begin{pmatrix} \cos\phi & 0 & \sin\phi \\ 0 & 1 & 0 \\ -\sin\phi & 0 & \cos\phi \end{pmatrix}. \tag{6}$$

Then, magnitudes of relevant mixing matrix elements to each mixing angle are

$$|U_{e2}| = \frac{1}{\sqrt{3}}, \quad |U_{e3}| = \left| \frac{2\sin\phi}{\sqrt{6}} \right|, \quad |U_{\mu 3}| = \left| -\frac{\sin\phi}{\sqrt{6}} + \frac{\cos\phi}{\sqrt{2}} \right|. \tag{7}$$

It can be seen that $\sin^2\theta_{12} > 1/3$ is predicted in this case,⁵ while the best fit value of $\sin^2\theta_{12}$ in a global analysis of the neutrino oscillation experiments tends to be lower than 1/3 [2].

⁵ This case can be easily realized in some actual flavor models [35, 36].

Another possibility of deviation from the TBM by an additional rotation is the 2–3 rotation from the TBM [9]. In the case, the PMNS mixing matrix is written as

$$U_{\text{PMNS}} = V_{\text{TBM}} \begin{pmatrix} 1 & 0 & 0 \\ 0 & \cos \phi & \sin \phi \\ 0 & -\sin \phi & \cos \phi \end{pmatrix}, \quad (8)$$

and the relevant mixing matrix elements are

$$|U_{e2}| = \left| \frac{\cos \phi}{\sqrt{3}} \right|, \quad |U_{e3}| = \left| \frac{\sin \phi}{\sqrt{3}} \right|, \quad |U_{\mu 3}| = \left| \frac{\sin \phi}{\sqrt{3}} + \frac{\cos \phi}{\sqrt{2}} \right|. \quad (9)$$

We find the upper limit on the magnitude of θ_{12} as $\sin^2 \theta_{12} < 1/3$, which is in favor of the current experimental results.

There also exists the last possibility of deviation constructed by an additional rotation to the TBM, i.e. 1-2 rotation, but this case does not lead to the non-zero θ_{13} . Therefore, we will focus on the additional 2-3 rotation and construct neutrino mass textures leading to the rotation, in the $(2 + 1)$ framework of the right-handed Majorana neutrinos described by the Eqs. (1) and (2) in the following sections.

3 Towards the minimal texture

We investigate neutrino mass matrix textures, which can lead to the additional 2-3 rotation to the TBM for the PMNS matrix, in the $(2 + 1)$ framework described by the Eqs. (1) and (2). Such framework can be applied to general models with the keV sterile neutrino DM, and required hierarchical mass spectrum of the right-handed Majorana neutrinos and the Yukawa couplings are partially realized by some mechanisms, e.g. the split seesaw mechanism [16]. As we mentioned above, the 2×2 right-handed Majorana neutrino mass matrix and the 3×2 Dirac neutrino mass matrix are effectively enough to give the flavor mixing and two mass squared differences of the neutrinos. Therefore, we focus on the structures of $M_R^{2 \times 2}$ and $Y_D^{3 \times 2}$ in the $(2 + 1)$ framework, the Eqs. (1) and (2).

We can take the 2×2 right-handed Majorana neutrino mass matrix $M_R^{2 \times 2}$ to be diagonal in general as follow:

$$M_R^{2 \times 2} = m_R \begin{pmatrix} \frac{1}{p} & 0 \\ 0 & 1 \end{pmatrix}, \quad (10)$$

where, m_R is a fundamental mass scale of the right-handed Majorana neutrino and p is a ratio between the two right-handed Majorana neutrino masses. On the other hand, the relevant Dirac neutrino mass matrix $M_D^{3 \times 2}$ is defined as

$$M_D^{3 \times 2} \equiv Y_D^{3 \times 2} v = \begin{pmatrix} a & d \\ b & e \\ c & f \end{pmatrix} v, \quad (11)$$

where $a \sim f$ are Yukawa couplings. By using the seesaw mechanism, the left-handed Majorana neutrino mass matrix M_ν can be well approximated by

$$M_\nu = M_D M_R^{-1} M_D^T \simeq M_D^{3 \times 2} (M_R^{2 \times 2})^{-1} (M_D^{3 \times 2})^T = \frac{v^2}{m_R} \begin{pmatrix} a^2 p + d^2 & abp + de & acp + df \\ abp + de & b^2 p + e^2 & bcp + ef \\ acp + df & bcp + ef & c^2 p + f^2 \end{pmatrix}, \quad (12)$$

in the decoupling limit of $M_R^{1 \times 1}$ for the light neutrino mass matrix Eq. (2). By performing the TBM matrix to the neutrino mass matrix M_ν , the left-handed Majorana neutrino mass matrix is rewritten as

$$M_\nu = \frac{v^2}{m_R} V_{\text{TBM}}^T \begin{pmatrix} \frac{A^2 p + D^2}{6} & \frac{ABp + DE}{3\sqrt{2}} & \frac{ACp + DF}{2\sqrt{3}} \\ \frac{ABp + DE}{3\sqrt{2}} & \frac{B^2 p + E^2}{3} & \frac{BCp + EF}{\sqrt{6}} \\ \frac{ACp + DF}{2\sqrt{3}} & \frac{BCp + EF}{\sqrt{6}} & \frac{C^2 p + F^2}{2} \end{pmatrix} V_{\text{TBM}}, \quad (13)$$

where

$$A \equiv 2a - b - c, \quad B \equiv a + b + c, \quad C \equiv c - b, \quad D \equiv 2d - e - f, \quad E \equiv d + e + f, \quad F \equiv f - e. \quad (14)$$

The Eq. (13) is called as the matrix in the TBM basis. We discuss neutrino mass structures to realize the additional 2-3 rotation for both cases of the normal and inverted neutrino mass hierarchies in sections 3.1 and 3.2, respectively.

3.1 Normal neutrino mass hierarchy

At first, we consider the case of the normal neutrino mass hierarchy (NH). It is seen that conditions for the additional 2-3 rotation are

$$A = 2a - b - c = 0, \quad D = 2d - e - f = 0. \quad (15)$$

After imposing these conditions on the Eq. (13), the mass matrix is rewritten as

$$M_\nu = \frac{v^2}{m_R} V_{\text{TBM}}^T \begin{pmatrix} 0 & 0 & 0 \\ 0 & \frac{3}{4}((b+c)^2 p + (e+f)^2) & \frac{1}{2}\sqrt{\frac{3}{2}}((c^2 - b^2)p - e^2 + f^2) \\ 0 & \frac{1}{2}\sqrt{\frac{3}{2}}((c^2 - b^2)p - e^2 + f^2) & \frac{1}{2}((b-c)^2 p + (e-f)^2) \end{pmatrix} V_{\text{TBM}}. \quad (16)$$

Since the Majorana neutrino mass can be rescaled in the seesaw formula, the right-handed Majorana and Dirac neutrino mass matrices are written by putting $p = 1$ as

$$M_R^{2 \times 2} = m_R \begin{pmatrix} 1 & 0 \\ 0 & 1 \end{pmatrix}, \quad M_D^{3 \times 2} = \begin{pmatrix} \frac{b+c}{2} & \frac{e+f}{2} \\ b & e \\ c & f \end{pmatrix} v, \quad (17)$$

respectively.⁶ Starting from these textures, we possibly simplify them in a context of texture zeros, which is one of attractive strategies to discuss minimal texture.

⁶ If one discuss a phenomenology depending on the right-handed Majorana neutrino masses, e.g. a generation mechanism of the BAU, one cannot rescale. However, such rescaling does not change our results of analyses for the mixing angles.

3.1.1 Two zero texture

Three or more texture zeros in the 3×2 Dirac neutrino mass matrix described by the Eq. (17) never give realistic lepton mixing angles consistent with the experimentally observed ones. Therefore, we begin with two zero texture. There are three cases for the two zero texture, in which possible conditions are

$$(i) \ b + c = 0, \ f = 0, \quad (ii) \ b + c = 0, \ e = 0, \quad (iii) \ c = 0, \ e = 0. \quad (18)$$

The other conditions give one vanishing mixing angle and lead only one non-vanishing neutrino mass. Now, corresponding Dirac neutrino mass matrices are given as

$$\frac{M_D^{3 \times 2}}{v} = \begin{cases} \begin{pmatrix} 0 & \frac{e}{2} \\ b & e \\ -b & 0 \end{pmatrix} & \text{for (i) } b + c = 0, \ f = 0 \\ \begin{pmatrix} 0 & \frac{f}{2} \\ b & 0 \\ -b & f \end{pmatrix} & \text{for (ii) } b + c = 0, \ e = 0 \ . \\ \begin{pmatrix} \frac{b}{2} & \frac{f}{2} \\ \frac{b}{2} & 0 \\ 0 & f \end{pmatrix} & \text{for (iii) } c = 0, \ e = 0 \end{cases} \quad (19)$$

It is also seen that resultant mixing angles will not be changed under the rescaling of $p = 1$ in the right-handed Majorana neutrino mass matrix and replacement between the first and the second columns of the Yukawa matrices in the right-hand side of the Eq. (19), but such replacement will lead to a wrong mass ratio $m_2/m_3 > 1$ as we will see later. Therefore, all patterns are included in the above three cases to be consistent with the experimental results.

We can express the 3×2 Dirac neutrino mass matrix in terms of only one parameter e or f by rescaling the overall factor v to m_0 and redefining rescaled $e \rightarrow e' = em_0/v$ or $f \rightarrow f' = fm_0/v$ as $e(\equiv e')$ and $f(\equiv f')$ without the loss of generality,

$$\frac{M_D^{3 \times 2}}{m_0} = \begin{cases} \begin{pmatrix} 0 & \frac{e}{2} \\ \frac{1}{\sqrt{2}} & e \\ -\frac{1}{\sqrt{2}} & 0 \end{pmatrix} & \text{for (i) } b + c = 0, \ f = 0 \\ \begin{pmatrix} 0 & \frac{f}{2} \\ \frac{1}{\sqrt{2}} & 0 \\ -\frac{1}{\sqrt{2}} & f \end{pmatrix} & \text{for (ii) } b + c = 0, \ e = 0 \ . \\ \begin{pmatrix} \frac{1}{2} & \frac{f}{2} \\ \frac{1}{2} & 0 \\ 0 & f \end{pmatrix} & \text{for (iii) } c = 0, \ e = 0 \end{cases} \quad (20)$$

(i) $\mathbf{b} + \mathbf{c} = \mathbf{0}$ and $\mathbf{f} = \mathbf{0}$ case

In the case (i), the left-handed Majorana neutrino is obtained as

$$M_\nu = \frac{m_0^2}{m_R} V_{\text{TBM}}^T \begin{pmatrix} 0 & 0 & 0 \\ 0 & \frac{3}{4}e^2 & -\frac{1}{2}\sqrt{\frac{3}{2}}e^2 \\ 0 & -\frac{1}{2}\sqrt{\frac{3}{2}}e^2 & 1 + \frac{1}{2}e^2 \end{pmatrix} V_{\text{TBM}}. \quad (21)$$

It can be seen that the additional 2-3 mixing angle, ϕ in the Eq. (8), is too large to be consistent with the experimental data if $e \sim \mathcal{O}(1)$. Therefore, we should take as $e \ll 1$. Then, the neutrino mass eigenvalues are

$$m_1 = 0, \quad \frac{m_2}{m_3} \simeq \frac{3}{4}e^2 \equiv r, \quad (22)$$

at the leading order, where r is around a ratio between two left-handed Majorana neutrino mass eigenvalues. The additional 2-3 mixing angle is

$$\tan(2\phi) \simeq -\sqrt{\frac{3}{2}}e^2, \quad (23)$$

where e is taken to be real for simplicity. The relevant mixing matrix elements are written from the Eqs. (22) and (23) as

$$|U_{e2}| \simeq \frac{1}{\sqrt{3}}\sqrt{1 - \frac{2}{3}r^2}, \quad |U_{e3}| \simeq \left| -\frac{\sqrt{2}}{3}r \right|, \quad |U_{\mu 3}| \simeq \left| -\frac{\sqrt{2}}{3}r + \frac{1}{\sqrt{2}}\sqrt{1 - \frac{2}{3}r^2} \right|. \quad (24)$$

We can find that the three mixing angles are correlated through the parameter r . The correlations among three mixing angles and predicted regions for each mixing angle are numerically shown in Fig. 1. In these numerical calculations, we take the parameter r to be complex as follows:

$$r = |r|e^{i\alpha}, \quad -\pi < \alpha < \pi. \quad (25)$$

Our numerical results of mixing angles should be compared to the experimental data [2] with 3σ as

$$0.27 \leq \sin^2 \theta_{12} \leq 0.37, \quad 0.36 \leq \sin^2 \theta_{23} \leq 0.68, \quad 0.017 \leq \sin^2 \theta_{13} \leq 0.033. \quad (26)$$

All plots are within 3σ ranges of both Δm_{atm}^2 and Δm_{sol}^2 [2] as

$$\Delta m_{\text{atm}}^2 = (2.55_{-0.24}^{+0.19}) \times 10^{-3} \text{ eV}^2, \quad \Delta m_{\text{sol}}^2 = (7.62_{-0.50}^{+0.58}) \times 10^{-5} \text{ eV}^2. \quad (27)$$

As seen from Figs. 1 (a) and 1 (b), we find that the case (i) is marginal to reproduce the experimental results, and we predict,

$$\begin{aligned} 0.320 \lesssim \sin^2 \theta_{12} \lesssim 0.322, \quad & 0.660 \lesssim \sin^2 \theta_{23} \lesssim 0.680, \\ 0.170 \text{ (0.130)} \lesssim \sin^2 \theta_{13} \text{ (}\sin \theta_{13}\text{)} \lesssim 0.196 \text{ (0.140)}. \end{aligned} \quad (28)$$

Two zero texture in the NH

(i) $b + c = 0$ and $f = 0$ case

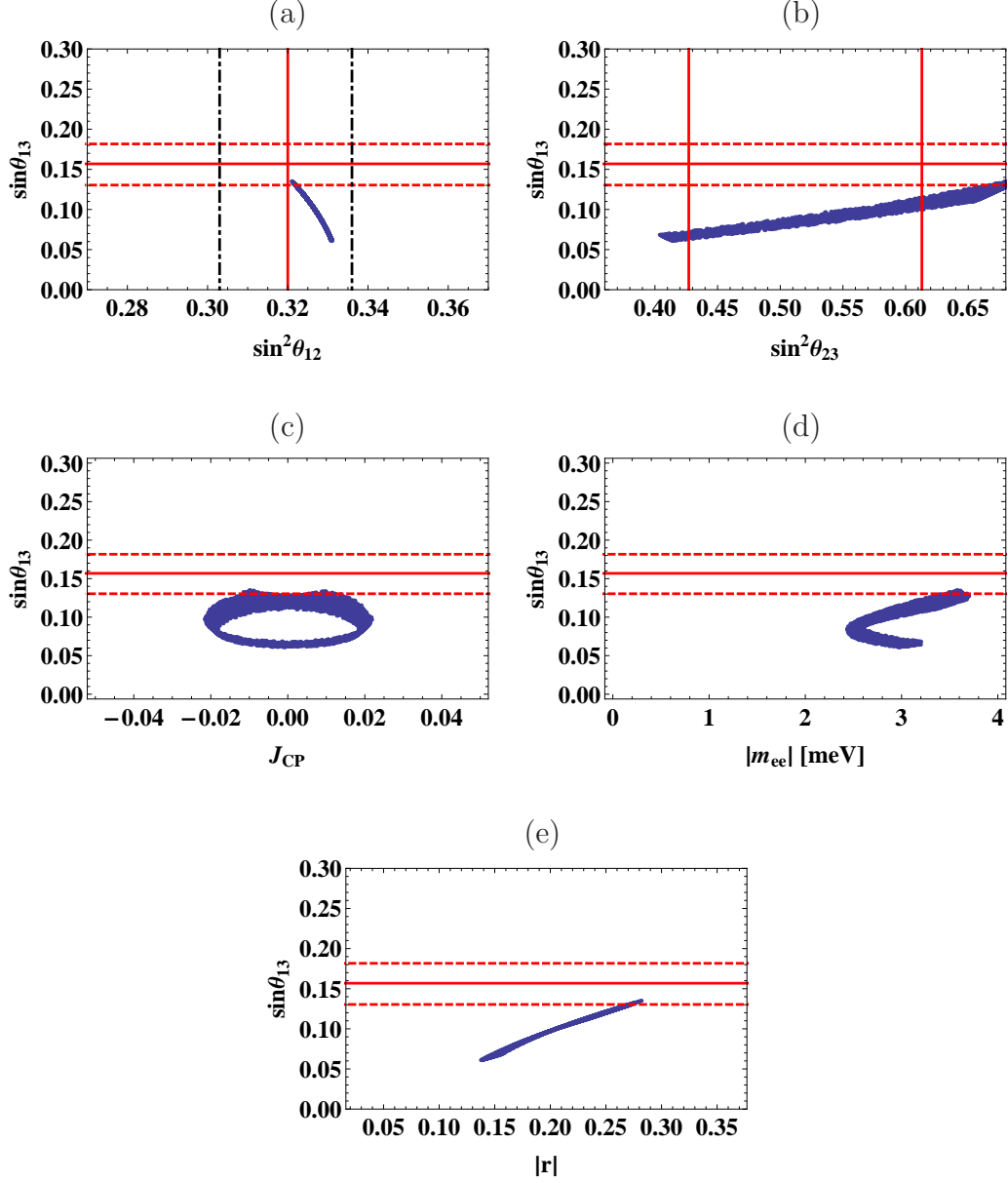


Figure 1: Predicted regions of mixing angles, the Jarlskog invariant, the effective neutrino mass for the $0\nu\beta\beta$, and a favored region of $|r|$ in the case (i) of NH with two zero texture: (a) $\sin^2\theta_{12}$ - $\sin\theta_{13}$, (b) $\sin^2\theta_{23}$ - $\sin\theta_{13}$, (c) J_{CP} - $\sin\theta_{13}$, (d) $|m_{ee}|$ - $\sin\theta_{13}$, and (e) $|r|$ - $\sin\theta_{13}$ planes. In the figures (a) and (b), the plots are within 3σ of the $\sin^2\theta_{23}$ and $\sin^2\theta_{12}$, respectively. In the figures (c), (d), and (e), the plots are within 3σ ranges of both $\sin^2\theta_{23}$ and $\sin^2\theta_{12}$. The best fit values of experimental data are denoted by solid lines in all figures. The chained and dashed lines denote experimental bounds of 1σ and 3σ , respectively.

Two zero texture in the NH

(ii) $b + c = 0$ and $e = 0$ case

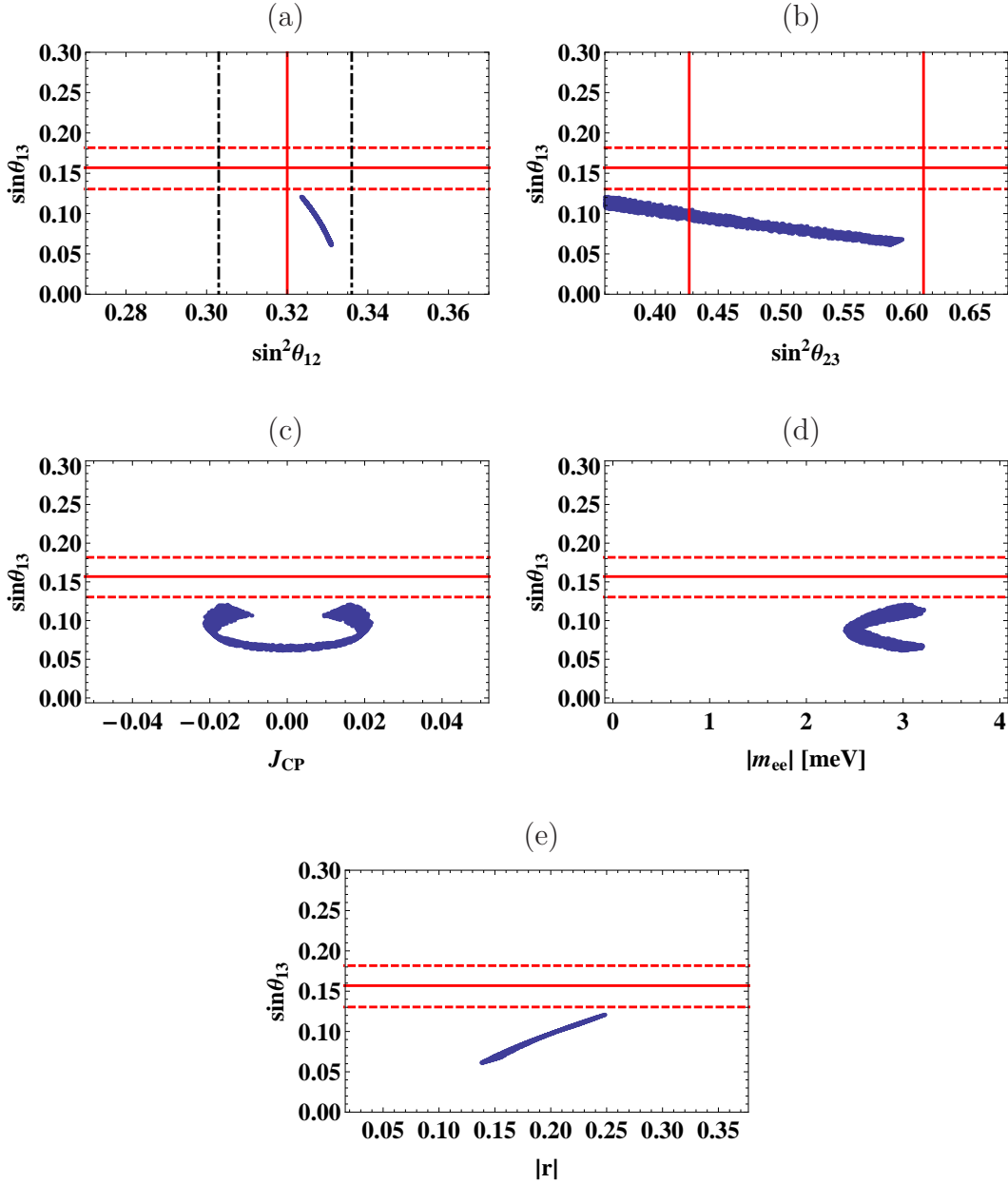


Figure 2: Predicted regions of mixing angles, the Jarlskog invariant, the effective neutrino mass for the $0\nu\beta\beta$, and a favored region of $|r|$ in the case (ii) of NH with two zero texture. The notations in each figure are the same as ones in the Fig. 1.

And the Jarlskog invariant, which is one of parameters describing the size of CP-violation, is predicted as

$$|J_{CP}| \equiv |\text{Im}(U_{\alpha i} U_{\beta j} U_{\beta i}^* U_{\alpha j}^*)| \simeq 0.01, \quad (29)$$

within the 3σ range of the θ_{13} in the Fig. 1 (c). The non-vanishing $|J_{CP}| = \mathcal{O}(0.01)$ promises an observation of the leptonic CP-violation in the future long-baseline neutrino experiments. An effective mass for the neutrino-less double beta decay ($0\nu\beta\beta$);

$$m_{ee} \equiv \sum_{i=1}^3 m_i U_{ei}^2, \quad (30)$$

is also predicted as

$$|m_{ee}| \simeq 3.6 \text{ meV}, \quad (31)$$

within the 3σ range of the θ_{13} in the Fig. 1 (d). The Heidelberg-Moscow experiment is currently giving the strongest bound on $|m_{ee}|$ as $|m_{ee}| \lesssim 210 \text{ meV}$ [37]. KamLAND-Zen has reported the bound $|m_{ee}| = (260 - 540) \text{ meV}$ [38], and will present the promising result in the near future. The KamLAND-Zen and CUORE experiments are expected to reach $|m_{ee}| \simeq (20 - 80) \text{ meV}$ [38] and $|m_{ee}| = (24 - 93) \text{ meV}$ [39], respectively. Thus, it may be difficult to check this texture by the future experiments.

In these numerical calculations, we have scanned over a broader range of $|r|$ ($0.02 \lesssim |r| \lesssim 0.4$) than a range expected by the Eqs. (22) and (27) within 3σ level to give complete predicted regions of physical quantities in the texture. It is actually found from the Fig. 1 (e) that a value around $r \sim \sqrt{\Delta m_{\text{sol}}^2 / \Delta m_{\text{atm}}^2}$ is favored by the experimental data.

(ii) $b + c = 0$ and $e = 0$ case

The left-handed Majorana neutrino mass matrix is

$$M_\nu = \frac{m_0^2}{m_R} V_{\text{TBM}}^T \begin{pmatrix} 0 & 0 & 0 \\ 0 & \frac{3}{4}f^2 & \frac{1}{2}\sqrt{\frac{3}{2}}f^2 \\ 0 & \frac{1}{2}\sqrt{\frac{3}{2}}f^2 & 1 + \frac{1}{2}f^2 \end{pmatrix} V_{\text{TBM}}. \quad (32)$$

It can be also seen that the additional mixing, ϕ , is too large to be consistent with the experimental data if $f \sim \mathcal{O}(1)$, and thus we must take $f \ll 1$ as well as $e \ll 1$ in the previous case (i). The neutrino mass eigenvalues and the additional mixing angle are

$$m_1 = 0, \quad \frac{m_2}{m_3} \simeq \frac{3}{4}f^2 \equiv r, \quad \tan(2\phi) \simeq \sqrt{\frac{3}{2}}f^2. \quad (33)$$

The relevant mixing matrix elements are written from the Eq. (33),

$$|U_{e2}| \simeq \frac{1}{\sqrt{3}}\sqrt{1 - \frac{2}{3}r^2}, \quad |U_{e3}| \simeq \frac{\sqrt{2}}{3}r, \quad |U_{\mu 3}| \simeq \left| \frac{\sqrt{2}}{3}r + \frac{1}{\sqrt{2}}\sqrt{1 - \frac{2}{3}r^2} \right|. \quad (34)$$

Results of numerical calculations for the mixing angles, the Jarlskog invariant, the effective mass, and the favored region of $|r|$ are shown in the Fig. 2. We find that this case cannot explain the current experimental results because the value of the $\sin \theta_{13}$ are not within 3σ range on the $\sin^2 \theta_{23}$ – $\sin \theta_{13}$ plane which is contrast to the case (i).

(iii) $c = 0$ and $e = 0$ case

The left-handed Majorana neutrino mass matrix is

$$M_\nu = \frac{m_0^2}{m_R} V_{\text{TBM}}^T \begin{pmatrix} 0 & 0 & 0 \\ 0 & \frac{3}{4}(f^2 + 1) & \frac{1}{2}\sqrt{\frac{3}{2}}(f^2 - 1) \\ 0 & \frac{1}{2}\sqrt{\frac{3}{2}}(f^2 - 1) & \frac{1}{2}(f^2 + 1) \end{pmatrix} V_{\text{TBM}}. \quad (35)$$

Since the neutrino mass eigenvalues can be obtained by

$$m_1 = 0, \quad \frac{m_2}{m_3} = \frac{5 + 5f^2 - \sqrt{25 - 46f^2 + 25f^4}}{5 + 5f^2 + \sqrt{25 - 46f^2 + 25f^4}} \equiv r, \quad (36)$$

the parameter f is evaluated as

$$f^2 \simeq \frac{25}{24}r \quad \text{or} \quad \frac{24}{25r}. \quad (37)$$

The additional mixing angle is

$$\tan(2\phi) = \frac{2\sqrt{6}(1 - f^2)}{1 + f^2} \simeq -2\sqrt{6} \quad \text{or} \quad 2\sqrt{6}, \quad (38)$$

and thus it is conflict with the experimental results because of the large additional rotation.

We conclude in this subsection that the case (i) is marginal to explain the experimental results but the cases of (ii) and (iii) are excluded.

3.1.2 One zero texture

Next, we discuss one zero textures leading to the additional 2-3 rotation to the TBM. There are three possible patterns of one zero texture as follows:

$$(I) \ b + c = 0, \quad (II) \ c = 0, \quad (III) \ b = 0, \quad (39)$$

in the Eq. (17). Corresponding Dirac neutrino mass matrices can be obtained as

$$\frac{M_D^{3 \times 2}}{m_0} = \begin{cases} \begin{pmatrix} 0 & \frac{e+f}{2} \\ \frac{1}{\sqrt{2}} & e \\ -\frac{1}{\sqrt{2}} & f \end{pmatrix} & \text{for (I) } b + c = 0 \\ \begin{pmatrix} \frac{1}{2} & \frac{e+f}{2} \\ 1 & e \\ 0 & f \end{pmatrix} & \text{for (II) } c = 0 \\ \begin{pmatrix} \frac{1}{2} & \frac{e+f}{2} \\ 0 & e \\ 1 & f \end{pmatrix} & \text{for (III) } b = 0 \end{cases}, \quad (40)$$

after rescaling in a similar way to the cases of two zero textures. However, in fact, all these patterns lead to exactly the same predictions for the mixing angles as we will show later. Therefore, we focus only on the texture of the case (I) $b + c = 0$ in detail.

Then, the right-handed Majorana and the Dirac neutrino mass matrices are written as

$$M_R^{2 \times 2} = m_R \begin{pmatrix} 1 & 0 \\ 0 & 1 \end{pmatrix}, \quad \frac{M_D^{3 \times 2}}{m_0} = \begin{pmatrix} 0 & \frac{e+f}{2} \\ \frac{1}{\sqrt{2}} & e \\ -\frac{1}{\sqrt{2}} & f \end{pmatrix}, \quad (41)$$

respectively. By using the seesaw mechanism, the left-handed Majorana neutrino mass matrix is

$$M_\nu = \frac{m_0^2}{m_R} \begin{pmatrix} \frac{1}{4}(e+f)^2 & \frac{1}{2}e(e+f) & \frac{1}{2}(e+f)f \\ \frac{1}{2}e(e+f) & \frac{1}{2} + e^2 & -\frac{1}{2} + ef \\ \frac{1}{2}(e+f)f & -\frac{1}{2} + ef & \frac{1}{2} + f^2 \end{pmatrix}. \quad (42)$$

In this case, the left-handed Majorana neutrino mass matrix is as follow:

$$M_\nu = \frac{m_0^2}{m_R} V_{\text{TBM}}^T \begin{pmatrix} 0 & 0 & 0 \\ 0 & \frac{3}{4}(e+f)^2 & -\frac{1}{2}\sqrt{\frac{3}{2}}(e-f)(e+f) \\ 0 & -\frac{1}{2}\sqrt{\frac{3}{2}}(e-f)(e+f) & 1 + \frac{1}{2}(e-f)^2 \end{pmatrix} V_{\text{TBM}}, \quad (43)$$

where we take the rescaled right-handed Majorana neutrino mass matrix as one given in the Eq. (17). When we take $e, f \ll 1$ to obtain appropriate size of the additional rotation, the neutrino mass eigenvalues are approximated by

$$m_1 = 0, \quad \frac{m_2}{m_3} \simeq \frac{3}{4}(e+f)^2 \equiv r. \quad (44)$$

As the result, the angle of the additional rotation is described by

$$\tan(2\phi) \simeq -\sqrt{\frac{3}{2}}(e-f)(e+f) \equiv \sqrt{6}\lambda. \quad (45)$$

Here it might be convenient for the following discussion to define new parameter, λ , as $\lambda \equiv \tan(2\phi)/\sqrt{6}$. In this case, relevant mixing matrix elements are given as

$$|U_{e2}| \simeq \sqrt{\frac{1}{3} - \frac{\lambda^2}{2}}, \quad |U_{e3}| \simeq \left| \frac{\lambda}{\sqrt{2}} \right|, \quad |U_{\mu 3}| \simeq \left| \frac{\lambda}{\sqrt{2}} + \sqrt{\frac{1}{2} - \frac{3\lambda^2}{4}} \right|. \quad (46)$$

Now, the parameters e and f can be reparameterized as

$$e = \frac{2re^{i\alpha} - 3\lambda e^{i\beta}}{2\sqrt{3}re^{i\alpha}}, \quad f = \frac{2re^{i\alpha} + 3\lambda e^{i\beta}}{2\sqrt{3}re^{i\alpha}}, \quad (47)$$

including phases with the Eq. (25) and

$$-\pi < \beta < \pi, \quad (48)$$

One zero texture in the NH

$$|\lambda| \leq 0.4$$

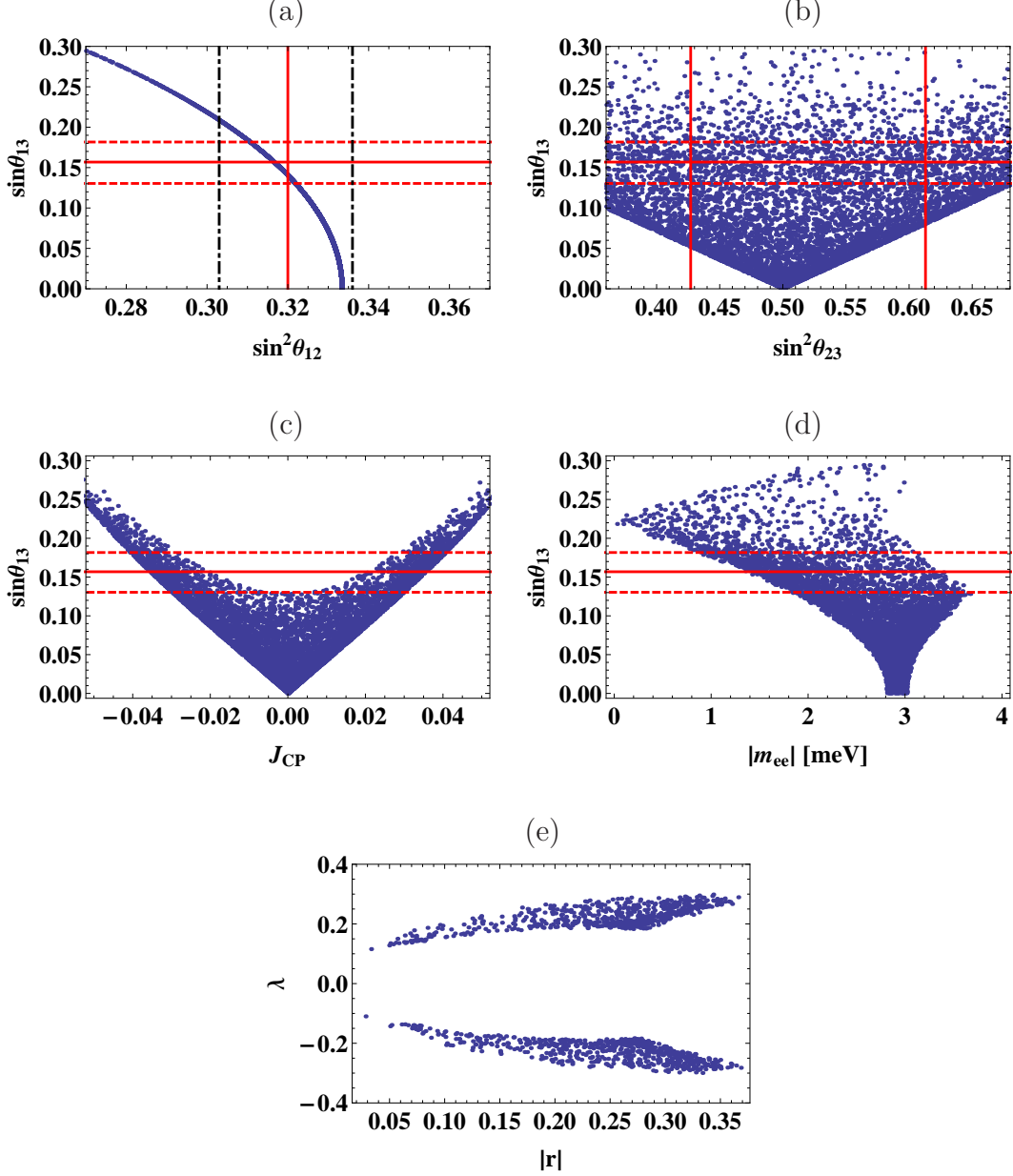


Figure 3: Predicted regions of mixing angles, the Jarlskog invariant, the effective neutrino mass for the $0\nu\beta\beta$, and a favored region of $|r|$ and λ in the one zero texture of NH. The other notations of each figure are the same as ones in the Fig. 1. The figure (e) is a plot on $|r|$ - λ plane where all points are within 3σ range of three mixing angles.

where we generically take e and f as complex. The parameters r and λ are real. We show the results of numerical calculation within the regions of parameters, the Eqs. (25), (48), and $|\lambda| \leq 0.4$. Since it is clear that relatively large value of $|\lambda|$, which determines the size of additional rotation, cannot be allowed by the experimental data, we scanned within a range of small values of $|\lambda|$. As seen in the Fig. 3 (a), there is a clear correlation between θ_{12} and θ_{13} . We predict

$$0.310 \lesssim \sin^2 \theta_{12} \lesssim 0.322, \quad (49)$$

within 3σ range of the $\sin \theta_{13}$, which is expected to be testable in the future precise neutrino experiments. On the other hand, there is no clear correlation between θ_{23} and θ_{13} because of the presence of two unknown phases (α and β) and complicated λ dependence of $|U_{\mu 3}|$ compared with $|U_{e2}|$ in the Fig. 3 (b). In the Figs. 3 (c) and 3 (d), $|J_{CP}|$ and $|m_{ee}|$ are also predicted as

$$|J_{CP}| \lesssim 0.04, \quad 0.8 \text{ meV} \lesssim |m_{ee}| \lesssim 3.6 \text{ meV}, \quad (50)$$

within 3σ range of the θ_{13} . A favored region of the parameters $|r|$ and λ is also shown in the Fig. 3 (e) where all points are within 3σ range of three mixing angles.

For the other possible cases of the one zero textures, (II) $c = 0$ and (III) $b = 0$, we can always take the same definitions of r and λ as ones in the case (I) without the loss of generality although forms of function for r and λ in terms of e and f are different among all cases. This means that predicted regions of the mixing angles, the Jarlskog invariant, and the effective neutrino mass for the $0\nu\beta\beta$ from three cases (I)-(III) are the same. Note that there are two free parameters r and λ to determine the neutrino mass ratio and the size of additional mixing angles in the one zero textures in contrast to the cases of the two zero textures, where each model described by only r , i.e. the additional mixing angles are tightly related with the neutrino mass ratio.

3.2 Inverted neutrino mass hierarchy

Let us discuss the case of the inverted neutrino mass hierarchy (IH). In order to lead to the additional 2-3 rotation, the (1, 2), (1, 3), (2, 1), and (3, 1) elements in the Eq. (13) should vanish. These conditions are given as

$$A = a + b + c = 0, \quad C = c - b, \quad D = 2d - e - f = 0. \quad (51)$$

Then, the left-handed Majorana neutrino mass matrix is written by

$$M_\nu = \frac{v^2}{m_R} V_{\text{TBM}}^T \begin{pmatrix} 6b^2p & 0 & 0 \\ 0 & \frac{3}{4}(e+f)^2 & -\frac{1}{2}\sqrt{\frac{3}{2}}(e-f)(e+f) \\ 0 & -\frac{1}{2}\sqrt{\frac{3}{2}}(e-f)(e+f) & \frac{1}{2}(e-f)^2 \end{pmatrix} V_{\text{TBM}}. \quad (52)$$

By reparameterizing of the matrix elements, we have

$$M_R^{2 \times 2} = m_R \begin{pmatrix} 1 & 0 \\ 0 & 1 \end{pmatrix}, \quad \frac{M_D^{3 \times 2}}{m_0} = \begin{pmatrix} -2 & \frac{e+f}{2} \\ 1 & e \\ 1 & f \end{pmatrix}. \quad (53)$$

The mass eigenvalues and the additional mixing angle are given by

$$m_3 = 0, \quad \frac{m_2}{m_1} = \frac{1}{24} (5e^2 + 2ef + 5f^2) \equiv r', \quad \tan \phi = \sqrt{\frac{2}{3}} \frac{e - f}{e + f}, \quad (54)$$

where e and f are supposed to be real, for simplicity, and the definition of r' differs from r in the NH case. Here note that if we consider one zero textures ($e = 0$, $f = 0$, or $e + f = 0$), the additional mixing becomes too large to be consistent with the experimental results. Therefore, we cannot consider zero textures for the Dirac neutrino mass matrix in the Eq. (53), and the texture of the Eq. (53) is a minimal one to lead to the additional 2-3 rotation to the TBM in the IH case.

In our calculations, we take e and f to be complex, and they are generically described by one complex number r' (with $|r'| > 1$) and one real number λ ($\equiv \tan(2\phi)/\sqrt{6}$) with phase β as $\lambda e^{i\beta}$. The results of numerical calculations are shown in the Fig. 4. All plots are within 3σ ranges of the experimental data [2] for the IH case as

$$\Delta m_{\text{atm}}^2 = -(2.43_{-0.22}^{+0.21}) \times 10^{-3} \text{ eV}^2, \quad \Delta m_{\text{sol}}^2 = (7.62_{-0.50}^{+0.58}) \times 10^{-5} \text{ eV}^2,$$

and should be also compared with the experimental data as

$$0.27 \leq \sin^2 \theta_{12} \leq 0.37, \quad 0.37 \leq \sin^2 \theta_{23} \leq 0.67, \quad 0.017 \leq \sin^2 \theta_{13} \leq 0.033. \quad (55)$$

We find that there is also a clear correlation between θ_{12} and θ_{13} shown in the Fig. 4 (a) as well as the NH case, and we predict

$$0.310 \lesssim \sin^2 \theta_{12} \lesssim 0.322, \quad (56)$$

within 3σ range of the $\sin \theta_{13}$. Further, it is also seen that there are some bounds, which come from the neutrino mass ratio, for three mixing angles as

$$0.276 \lesssim \sin^2 \theta_{12}, \quad 0.400 \lesssim \sin^2 \theta_{23}, \quad \sin^2 \theta_{13} (\sin \theta_{13}) \lesssim 0.0784 (0.280), \quad (57)$$

in the contrast to the case (I) of NH with one zero texture shown in the Fig. 3. We also predict

$$0.01 \lesssim |J_{CP}| \lesssim 0.04, \quad 42 \text{ meV} \lesssim |m_{ee}| \lesssim 51 \text{ meV}, \quad (58)$$

within 3σ range of the θ_{13} in the Figs. 4 (c) and 4 (d). These predictions are expected to be testable in the future precise neutrino experiments. Especially, the effective mass in this IH case might be measured by the future KamLAND-Zen and CUORE experiments.

Also in these numerical calculations, we have scanned over a broader range of $|r'|$ ($1 < |r'| \lesssim 1.2$) than a range expected by the Eqs. (54) and (55) within 3σ level to present complete predicted regions of physical quantities from this texture. It is also seen from the Fig. 4 (e) that a value around $r' \sim \sqrt{(\Delta m_{\text{atm}}^2 + \Delta m_{\text{sol}}^2)/\Delta m_{\text{atm}}^2}$ is favored by the experimental results.

$$|\lambda| \leq 0.4$$

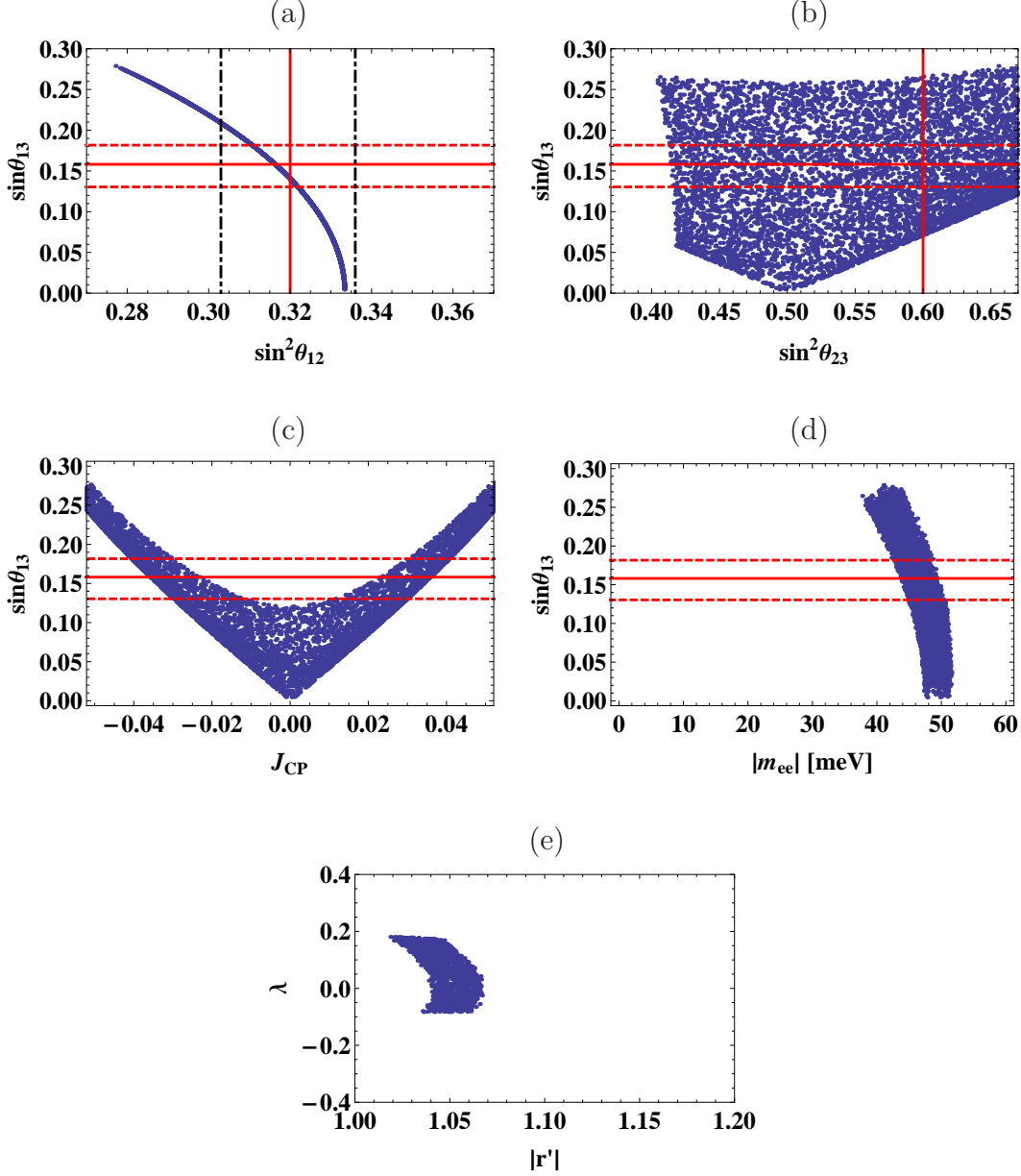


Figure 4: Predicted regions of mixing angles, the Jarlskog invariant, the effective neutrino mass for the $0\nu\beta\beta$, and a favored region of $|r|$ and λ in the minimal texture of the IH. The notations of each figure are the same as ones in the Fig. 1. The figure (e) is a plot on $|r'|$ - λ plane where all points are within 3σ range of three mixing angles.

4 Texture with Cabibbo angle and neutrino mass ratio

In the previous sections, we have presented relatively general discussions of 3×2 textures for the Dirac neutrino mass matrix (with zeros) in the context of (2+1) seesaw mechanism. At the end of this work, we consider interesting textures with specific assumptions and show their predictions. A basic strategy to make assumptions is to regard some small parameters in our context as the Cabibbo angle or the neutrino mass ratio. The reasons for such identification are just that it is now phenomenologically allowed in the current stage of neutrino oscillation experiments. We will not construct some actual high energy models to make the assumption valid in this work but such kind of assumptions might well motivate for studies of theory and/or symmetry in the quark/lepton sectors behind the SM. Here we still concentrate on texture analyses with the above assumptions.

In the previous sections, we investigate two and one zero textures. In the two zero textures, the model is described by one parameter r after rescaling the right-handed Majorana neutrino mass matrix. Then, the parameter r is approximated by the ratio between two mass squared differences of neutrino and determines the size of additional 2-3 mixing angle ϕ . As the results we predict some clearly correlated regions of the mixing angles. On the other hand, in the one zero textures, we have one more parameter λ in addition to r , which characterize the models. The λ determines the magnitude of the additional mixing angle and it is restricted to be small by the current experimental data. In this section, we consider the model of one zero texture with the assumptions that the parameter λ is identified with the Cabibbo angle or the related parameter with the neutrino mass ratio.

4.1 One zero texture with the Cabibbo angle

First, we discuss the case that the model parameter λ in the Eq. (45) is taken as the Cabibbo angle, $\lambda = 0.225$. The numerical calculation of the case is given in the Fig. 5 and should be compared with the case in the Fig. 3. The same numerical setup for the other parameter apart from λ is taken as ones in the section 3.1.2. In the Fig. 5 (a), the $\sin^2 \theta_{12}$ and $\sin^2 \theta_{13}$ ($\sin \theta_{13}$) are predicted as

$$\sin^2 \theta_{12} \simeq 0.315, \quad \sin^2 \theta_{13} (\sin \theta_{13}) \simeq 0.0272 (0.165), \quad (59)$$

which are close to the best fit values in the current experimental data. On the other hand, we cannot predict the value of the $\sin^2 \theta_{23}$ as seen the Fig. 5 (b). Regarding with the J_{CP} and $|m_{ee}|$, they are predicted as

$$0.02 \lesssim |J_{CP}| \lesssim 0.04, \quad 1.2 \text{ meV} \lesssim |m_{ee}| \lesssim 3.4 \text{ meV}, \quad (60)$$

within 3σ range of the θ_{13} in the Figs. 5 (c) and 5 (d). Such a large J_{CP} is expected to be measured in the future long-baseline neutrino experiments. The Fig. 5 (e) is a plot on $|r|-\lambda$ plane where all points are within 3σ range of three mixing angles. This kind of model such that the additional rotation is described by the Cabibbo angle might be constructed by a high energy theory or symmetry for quark-lepton sectors.

One zero texture with the Cabibbo angle and neutrino mass ratio in the NH

$$\lambda = 0.225$$

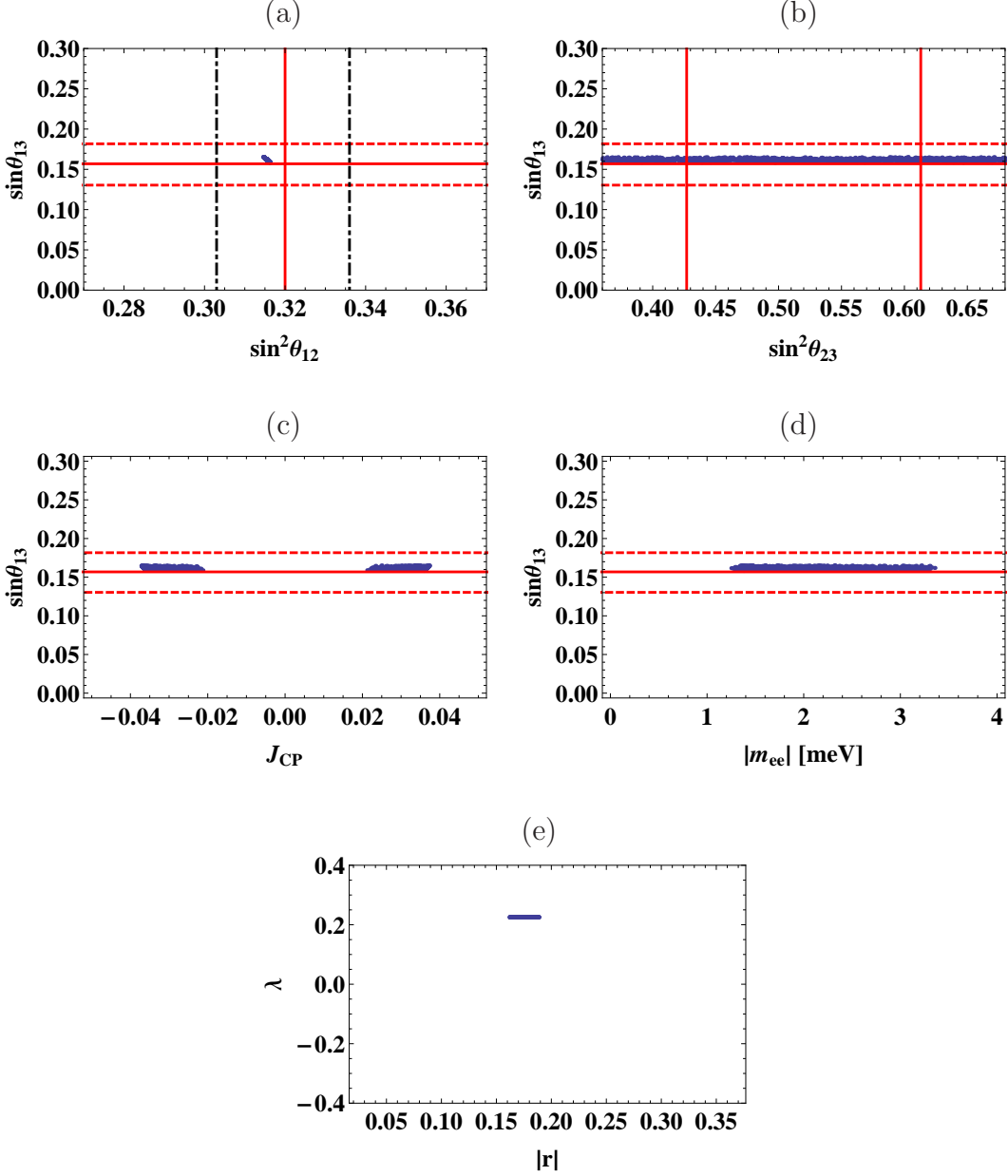


Figure 5: Predicted regions of mixing angles, the Jarlskog invariant, the effective neutrino mass for the $0\nu\beta\beta$, and a favored region of $|r|$ and λ in the one zero texture with $\lambda = 0.225$. The notations of each figure are the same as ones in the Fig. 1. The figure (e) is a plot on $|r|$ - λ plane where all points are within 3σ range of three mixing angles.

One zero texture with the Cabibbo angle and neutrino mass ratio in the NH

$$\lambda/\sqrt{2} = r$$

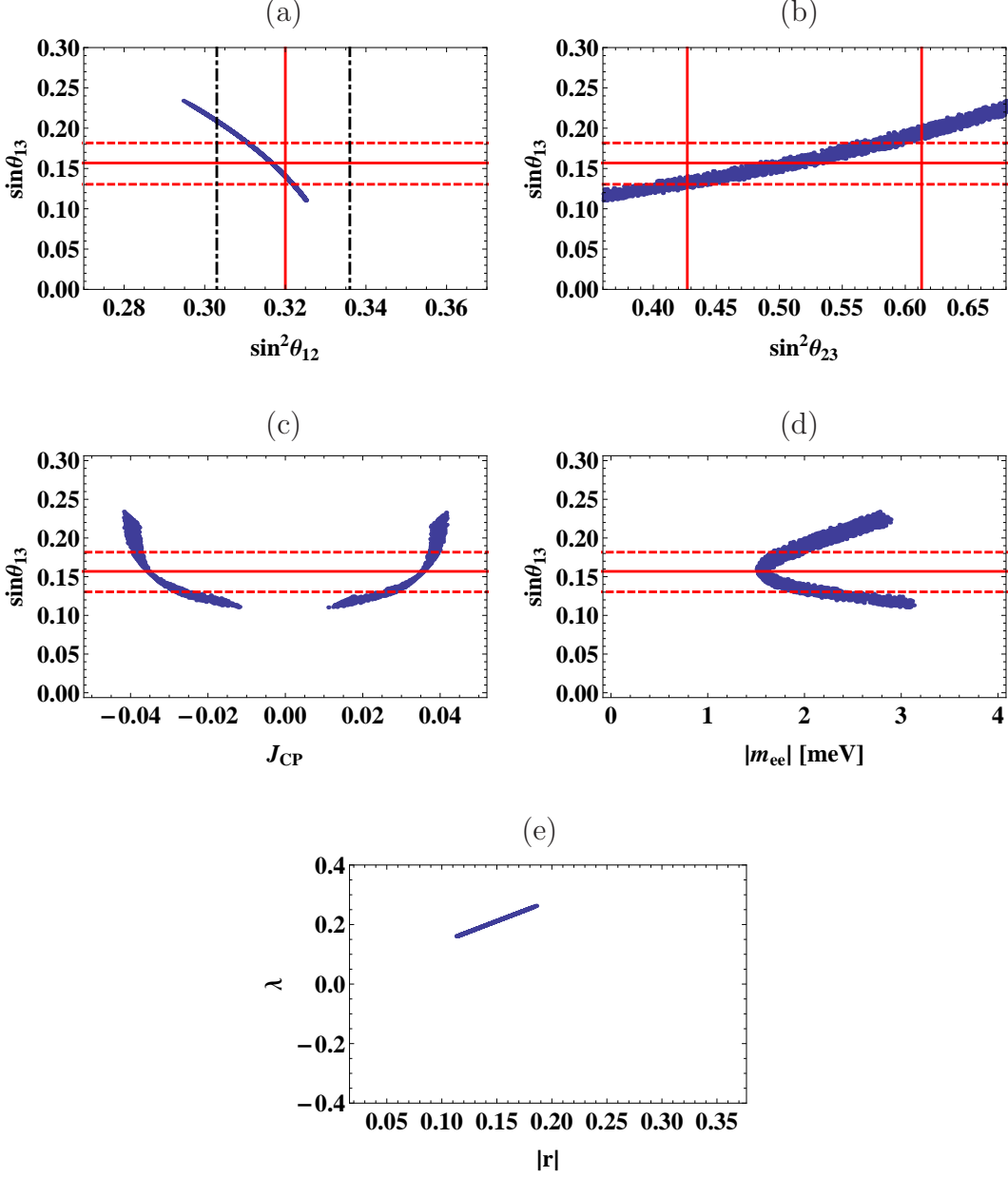


Figure 6: Predicted regions of mixing angles, the Jarlskog invariant, the effective neutrino mass for the $0\nu\beta\beta$, and a favored region of $|r|$ and λ in the one zero texture with $\lambda/\sqrt{2} = r$. The notations of each figure are the same as ones in the Fig. 1. The figure (e) is a plot on $|r|$ - λ plane where all points are within 3σ range of three mixing angles.

4.2 One zero texture with the neutrino mass ratio

The next concern is to investigate the one zero texture including only one small parameter as well as the two zero texture case, i.e. λ is also related with the ratio between two mass squared differences of neutrinos because the ratio is naturally appeared in neutrino mass models.

We take $\lambda/\sqrt{2} = r$ in the Eq. (47). In the case, the neutrino mass matrix is generally described one (complex) parameter, r .⁷ The results of numerical calculation are shown in the Fig. 6 with $\lambda/\sqrt{2} = r$ and should be compared to the case in the Fig. 3 and Fig. 5 with $\lambda = 0.225$. The same numerical setup for the other parameter apart from λ is taken as ones in the section 3.1.2. We predict

$$\begin{aligned} 0.310 \lesssim \sin^2 \theta_{12} \lesssim 0.322, \quad 0.380 \lesssim \sin^2 \theta_{23} \lesssim 0.600, \\ 0.02 \lesssim |J_{CP}| \lesssim 0.04, \quad 1.5 \text{ meV} \lesssim |m_{ee}| \lesssim 2.7 \text{ meV}, \end{aligned} \quad (61)$$

within 3σ range of the $\sin \theta_{13}$ from the Fig. 6 (a) to 6 (d). The J_{CP} is expected to be measured in the future long-baseline neutrino experiments. The Fig. 6 (e) is a plot on $|r|-\lambda$ plane where all points are within 3σ range of three mixing angles.

5 Summary

We have presented neutrino mass matrix textures in the minimal framework of the type-I seesaw mechanism where two right-handed Majorana neutrinos are introduced in order to reproduce the experimental results of neutrino oscillations. The textures can lead to experimentally favored leptonic mixing angles described by the TBM and the additional 2-3 rotation. The setup can be generically embedded into some scenarios with e.g. the keV sterile neutrino DM.

First, we have presented minimal textures with two zeros in the Dirac neutrino mass matrix for the NH case. In the case with two zeros, there are possibly three patterns for the position of zero in the Dirac neutrino mass matrix. The textures in this case is described by only one free parameter r , which should be around the ratio between the neutrino mass squared differences. We have shown that one of three is marginal to explain the experimental results while the others are ruled out because the free parameter is severely restricted. The predictions from the possible texture are $0.320 \lesssim \sin^2 \theta_{12} \lesssim 0.322$, $0.660 \lesssim \sin^2 \theta_{23} \lesssim 0.680$, 0.170 (0.130) $\lesssim \sin^2 \theta_{13}$ ($\sin \theta_{13} \lesssim 0.196$ (0.140)), and $|J_{CP}| \simeq 0.01$ and $|m_{ee}| \simeq 3.6$ meV within 3σ range of the θ_{13} .

Next, we have shown (next to minimal) textures with one zero for the NH. It has been shown that there are three possible patterns for the position of zero as well as the two zero textures but all three textures with one zero lead to the same predictions for θ_{ij} , J_{CP} , and m_{ee} because the same definitions of two model parameters (r and λ) can be taken for all three cases without the loss of generality. This is one of different properties between the two and one zero(s) textures. We could not predict values of θ_{23} and θ_{13} but find a clear

⁷The factor $\sqrt{2}$ in $\lambda/\sqrt{2} = r$ may also be interesting if r and λ are just taken as the neutrino mass ratio, $r = m_2/m_3 = \sqrt{\Delta m_{\text{sol}}^2/\Delta m_{\text{atm}}^2} \simeq 0.16$, and as the Cabibbo angle, $\lambda/\sqrt{2} \simeq 0.225/\sqrt{2} \simeq 0.16$, respectively.

correlation between θ_{12} and θ_{13} . The predictions from the texture are $0.310 \lesssim \sin^2 \theta_{12} \lesssim 0.322$, $|J_{CP}| \lesssim 0.04$, and $0.8 \text{ meV} \lesssim |m_{ee}| \lesssim 3.6 \text{ meV}$ within 3σ range of θ_{13} .

Then, the IH case has been also investigated. In this case, textures with zero(s) is conflicts with the experimental results. Therefore, we have constructed a texture described by two free parameters without zero. The predictions from the texture are $0.310 \lesssim \sin^2 \theta_{12} \lesssim 0.322$, $0.01 \lesssim |J_{CP}| \lesssim 0.04$, and $42 \text{ meV} \lesssim |m_{ee}| \lesssim 51 \text{ meV}$ within 3σ range of the θ_{13} . The result of $|m_{ee}|$ might be tested by the future KamLAND-Zen and CUORE experiments of the $0\nu\beta\beta$. We could also find some limits for three mixing angles as $0.276 \lesssim \sin^2 \theta_{12}$, $0.400 \lesssim \sin^2 \theta_{23}$, and $\sin^2 \theta_{13}$ ($\sin \theta_{13}$) $\lesssim 0.0784$ (0.280) in the contrast to the NH case with the one zero texture.

Finally, we have considered the model of the one zero texture with the assumptions that one of model parameters is related to the Cabibbo angle or the ratio between mass squared differences of the neutrinos. These assumptions are now phenomenologically allowed and might be motivated for studies of theory and/or symmetry in the quark/lepton sectors behind the SM. The first concern was the case with the assumption that the model parameter λ is the Cabibbo angle. In the case, we could not still predict values of the θ_{23} but find $\sin^2 \theta_{12} \simeq 0.315$ and $\sin^2 \theta_{13}$ ($\sin \theta_{13}$) $\simeq 0.0272$ (0.165). For J_{CP} and $|m_{ee}|$, $0.02 \lesssim |J_{CP}| \lesssim 0.04$ and $1.2 \text{ meV} \lesssim |m_{ee}| \lesssim 3.4 \text{ meV}$ are predicted within 3σ range of the θ_{13} . In the second one such that the parameter is taken as $\lambda/\sqrt{2} = r$, we have found $0.310 \lesssim \sin^2 \theta_{12} \lesssim 0.322$, $0.380 \lesssim \sin^2 \theta_{23} \lesssim 0.600$, $0.02 \lesssim |J_{CP}| \lesssim 0.04$, and $1.5 \text{ meV} \lesssim |m_{ee}| \lesssim 2.7 \text{ meV}$ within 3σ range of the θ_{13} . This case of $\lambda/\sqrt{2} = r$ may be more interesting if r and λ are just taken as the neutrino mass ratio, $r = m_2/m_3 = \sqrt{\Delta m_{\text{sol}}^2/\Delta m_{\text{atm}}^2} \simeq 0.16$, and as the Cabibbo angle, $\lambda/\sqrt{2} \simeq 0.225/\sqrt{2} \simeq 0.16$, respectively.

All our results are expected to be comprehensively tested by combining results from more precise determinations of mixing angles, leptonic CP-violation searches, and the $0\nu\beta\beta$ experiments in the future.

Acknowledgment

We thank W. Rodejohann for useful comments. The work of R.T. are supported by Research Fellowships of the Japan Society for the Promotion of Science (JSPS) for Young Scientists. M.T. is supported by JSPS Grand-in-Aid for Scientific Research, 21340055 and 24654062.

References

- [1] F. P. An *et al.* [DAYA-BAY Collaboration], Phys. Rev. Lett. **108** (2012) 171803 [arXiv:1203.1669 [hep-ex]].
- [2] D. V. Forero, M. Tortola and J. W. F. Valle, arXiv:1205.4018 [hep-ph].
- [3] G. L. Fogli, E. Lisi, A. Marrone, D. Montanino, A. Palazzo and A. M. Rotunno, Phys. Rev. D **86** (2012) 013012 [arXiv:1205.5254 [hep-ph]].
- [4] M. C. Gonzalez-Garcia, M. Maltoni, J. Salvado and T. Schwetz, arXiv:1209.3023 [hep-ph].

- [5] P. F. Harrison, D. H. Perkins, W. G. Scott, Phys. Lett. B **530** (2002) 167 [hep-ph/0202074].
- [6] P. F. Harrison, W. G. Scott, Phys. Lett. B **535** (2002) 163-169 [hep-ph/0203209].
- [7] H. Ishimori, T. Kobayashi, H. Ohki, Y. Shimizu, H. Okada and M. Tanimoto, Prog. Theor. Phys. Suppl. **183** (2010) 1 [arXiv:1003.3552 [hep-th]].
- [8] H. Ishimori, T. Kobayashi, H. Ohki, H. Okada, Y. Shimizu and M. Tanimoto, Lect. Notes Phys. **858** (2012) 1.
- [9] W. Rodejohann and H. Zhang, arXiv:1207.1225 [hep-ph].
- [10] A. Damanik, arXiv:1206.0987 [hep-ph].
- [11] S. F. King, arXiv:1205.0506 [hep-ph].
- [12] Y. Shimizu and R. Takahashi, Europhys. Lett. **93** (2011) 61001 [arXiv:1009.5504 [hep-ph]].
- [13] P. Minkowski, Phys. Lett. B **67** (1977) 421; T. Yanagida, in Proceedings of the Workshop on Unified Theories and Baryon Number in the Universe, eds. O. Sawada and A. Sugamoto (KEK report 79-18, 1979); M. Gell-Mann, P. Ramond and R. Slansky, in Supergravity, eds. P. van Nieuwenhuizen and D.Z. Freedman (North Holland, Amsterdam, 1979); R. N. Mohapatra and G. Senjanovic, Phys. Rev. Lett. **44** (1980) 912; J. Schechter and J. W. F. Valle, Phys. Rev. D **22** (1980) 2227; J. Schechter and J. W. F. Valle, Phys. Rev. D **25** (1982) 774.
- [14] T. Asaka, S. Blanchet and M. Shaposhnikov, Phys. Lett. B **631** (2005) 151 [hep-ph/0503065].
- [15] T. Asaka and M. Shaposhnikov, Phys. Lett. B **620** (2005) 17 [hep-ph/0505013].
- [16] A. Kusenko, F. Takahashi and T. T. Yanagida, Phys. Lett. B **693** (2010) 144 [arXiv:1006.1731 [hep-ph]].
- [17] J. Barry, W. Rodejohann and H. Zhang, JCAP **1201** (2012) 052 [arXiv:1110.6382 [hep-ph]].
- [18] C. -S. Chen and R. Takahashi, Eur. Phys. J. C **72** (2012) 2089 [arXiv:1112.2102 [hep-ph]].
- [19] C. D. Froggatt and H. B. Nielsen, Nucl. Phys. B **147** (1979) 277.
- [20] A. Merle and V. Niro, JCAP **1107** (2011) 023 [arXiv:1105.5136 [hep-ph]].
- [21] M. Lindner, A. Merle and V. Niro, JCAP **1101** (2011) 034 [arXiv:1011.4950 [hep-ph]].
- [22] S. F. King, Phys. Lett. B **439** (1998) 350 [hep-ph/9806440].

- [23] S. F. King, Nucl. Phys. B **562** (1999) 57 [hep-ph/9904210].
- [24] G. C. Branco, R. Gonzalez Felipe, F. R. Joaquim and T. Yanagida, Phys. Lett. B **562** (2003) 265 [hep-ph/0212341].
- [25] P. H. Frampton, S. L. Glashow and T. Yanagida, Phys. Lett. B **548** (2002) 119 [hep-ph/0208157].
- [26] S. Goswami and A. Watanabe, Phys. Rev. D **79** (2009) 033004 [arXiv:0807.3438 [hep-ph]].
- [27] S. Goswami, S. Khan and A. Watanabe, Phys. Lett. B **693** (2010) 249 [arXiv:0811.4744 [hep-ph]].
- [28] W. Rodejohann, M. Tanimoto and A. Watanabe, Phys. Lett. B **710** (2012) 636 [arXiv:1201.4936 [hep-ph]].
- [29] K. Harigaya, M. Ibe and T. T. Yanagida, Phys. Rev. D **86** (2012) 013002 [arXiv:1205.2198 [hep-ph]].
- [30] K. Bhattacharya, N. Sahu, U. Sarkar and S. K. Singh, Phys. Rev. D **74** (2006) 093001 [hep-ph/0607272].
- [31] A. Adulpravitchai and R. Takahashi, JHEP **1109** (2011) 127 [arXiv:1107.3829 [hep-ph]].
- [32] J. Beringer *et al.* [Particle Data Group Collaboration], Phys. Rev. D **86** (2012) 010001.
- [33] Z. Maki, M. Nakagawa and S. Sakata, Prog. Theor. Phys. **28** (1962) 870.
- [34] B. Pontecorvo, Sov. Phys. JETP **26** (1968) 984 [Zh. Eksp. Teor. Fiz. **53** (1967) 1717].
- [35] H. Ishimori, Y. Shimizu, M. Tanimoto and A. Watanabe, Phys. Rev. D **83** (2011) 033004 [arXiv:1010.3805 [hep-ph]].
- [36] Y. Shimizu, M. Tanimoto and A. Watanabe, Prog. Theor. Phys. **126** (2011) 81 [arXiv:1105.2929 [hep-ph]].
- [37] H. V. Klapdor-Kleingrothaus, A. Dietz, L. Baudis, G. Heusser, I. V. Krivosheina, S. Kolb, B. Majorovits and H. Pas *et al.*, Eur. Phys. J. A **12** (2001) 147 [hep-ph/0103062].
- [38] A. Gando *et al.* [KamLAND-Zen Collaboration], Phys. Rev. C **85** (2012) 045504 [arXiv:1201.4664 [hep-ex]]; K. Inoue [KamLAND-Zen Collaboration], talk slide at Neutrino 2012.
- [39] C. Arnaboldi *et al.* [CUORE Collaboration], Nucl. Instrum. Meth. A **518** (2004) 775 [hep-ex/0212053]; M. Sisti [CUORE Collaboration], J. Phys. Conf. Ser. **203** (2010) 012069; F. Bellini, C. Bucci, S. Capelli, O. Cremonesi, L. Gironi, M. Martinez, M. Pavan and C. Tomei *et al.*, Astropart. Phys. **33** (2010) 169 [arXiv:0912.0452 [physics.ins-det]].